ELECTRONIC SUPPLEMENTARY MATERIAL

Marangoni Bursting: Insight into the Role of the Thermocapillary Effect in an Oil Bath

Michalina Ślemp [1,2] and Andrzej Miniewicz [1,*]

[1] Institute of Advanced Materials, Faculty of Chemistry, Wroclaw University of Science and Technology, Wybrzeze Wyspianskiego 27, 50-370 Wroclaw, Poland; e-mail: andrzej.miniewicz@pwr.edu.pl
[2] Non-Linear Optical and Interfaces Group, Institute of Light and Matter, Uinveristy Claude Bernard Lyon 1, Villeurbane, France; e-mail: michalina.slemp@gmail.com
* Correspondence: andrzej.miniewicz@pwr.edu.pl; (A.M.)

1. Description of videos referenced in the main manuscript (.mp4 files)

Video S1. Typical Marangoni bursting process observed via thermal camera FLIR E96 for initial IPA content in H_2O $\phi_0 = 0.4$ (with dissolved methyl blue dye) on pure rapeseed oil. Intense blue color corresponds to temperature lower approximately by 5 K than room temperature of oil phase (yellow color), respectively. The movie is shown in a real time.

Video S2. Marangoni bursting process observed via thermal camera FLIR E96 for initial IPA content in H_2O $\phi_0 = 0.45$ (with methyl blue dye) deposited on pure rapeseed oil. Blue color here denotes lower temperature and yellow higher temperature, respectively. Note the formation of outer and inner rims in the final phase of the phenomenon. This effect is explained in the main manuscript. The movie is shown in a real time and its duration is 54 s.

Video S3. Enlarged view of Marangoni bursting observed via thermal camera FLIR E96 for initial IPA content in H_2O $\phi_0 = 0.5$ (with methyl blue dye) on pure rapeseed oil. Blue color here denotes lower temperature and yellow higher temperature, respectively. The period of fingering instability λ decreases with increase of alcohol content in the initial binary solution. Note the formation of outer rim that moves toward the center. In the center temperature is increasing while at the periphery it remains low – possibly due to water evaporation. The movie is shown at doubled speed with respect to a real time.

Video S4. Marangoni bursting observed via thermal camera FLIR E96 for the initial IPA content in H_2O $\phi_0 = 0.6$. Blue color here denotes lower temperature and yellow higher temperature, respectively. Note the continuous decrease in fingering instability wavelength λ. The movie is shown in a real time.

Video S5. Marangoni bursting observed via thermal camera FLIR E96 for initial IPA content in H_2O ϕ_0 = 0.7 (with methyl blue dye) on pure rapeseed oil. Blue color here denotes lower temperature and yellow higher temperature, respectively. Note the further decrease in instability wavelength λ. The peripheric rim movement velocity toward the center can easily be determined. The movie is shown at doubled speed with respect to a real time.

2. Supplementary results

Dynamic surface temperature measurements using FLIR camera during Marangoni bursting allowed to estimate the temperature gradients and their evolution in time. The gradients result from alcohol and water evaporation during the whole process. An example of temperature differences across the expanding mother droplet accompanied with fingering instability is shown in Figure S1.

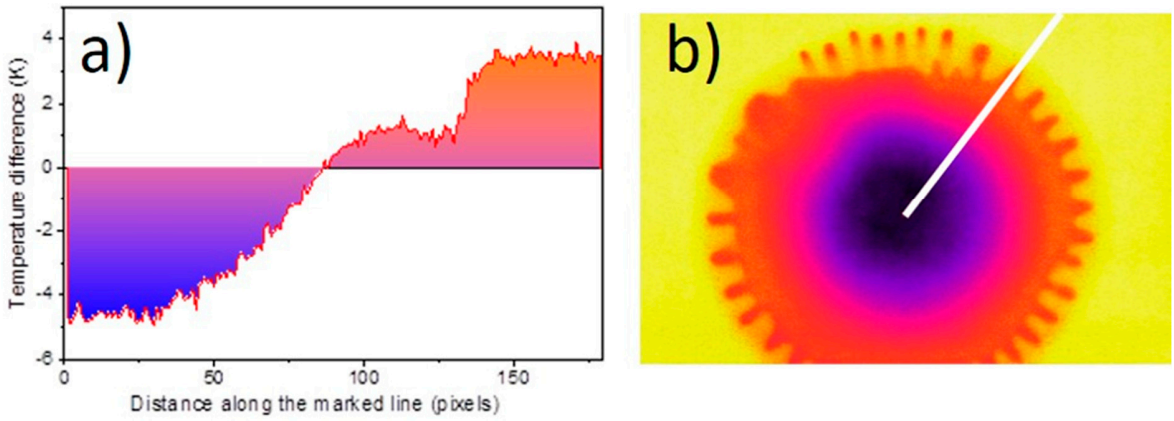

Figure S1. (a) Surface temperature differences across the white line (see Figure S1b) for mother droplet of alcohol and water (ϕ_0 = 0.45) spreading over oil bath surface. Note that the total temperature difference between droplet center and the free oil phase amounts to ~ 7.5 K. (b) A temperature map captured in the initial stage of mother droplet spreading. Note that the leading edge of a finger shows a slightly lower temperature than in the area where fingers are not present.

In Figure S2 the surface temperature differences measured along daughter droplets after their detachment from mother droplet in Marangoni bursting phenomenon are shown. The red line is drawn along a row of the 6 consecutive droplets moving at the oil pool surface toward the periphery. The temperature assigned to this line is shown in Figure S2b. Two characteristic features can be noticed: (i) after mother droplet disappearance the temperature measured at the center is higher than that at the periphery (see the temperature envelope in Figure S2b); (ii) at each droplet

position (shown in Figure S2 by numbers 1 to 6) there is a considerable sharp temperature decrease amounting on average 1.3 K. For daughter droplets with numbers 2, 3, 4 and 6 one can notice minute temperature decrease (0.2 K at average) associated with the position of the droplet leading edge in the movement toward the periphery. This suggests that spreading makes the droplet front thinner than its rear. Therefore, alcohol evaporation is faster at the droplet front thus making Marangoni thermocapillary flows to be directed toward this cooler side of the droplet. With time when the amount of alcohol drops (see droplet 6) the Marangoni stress is vanishing and droplets slow-down in their motion toward periphery.

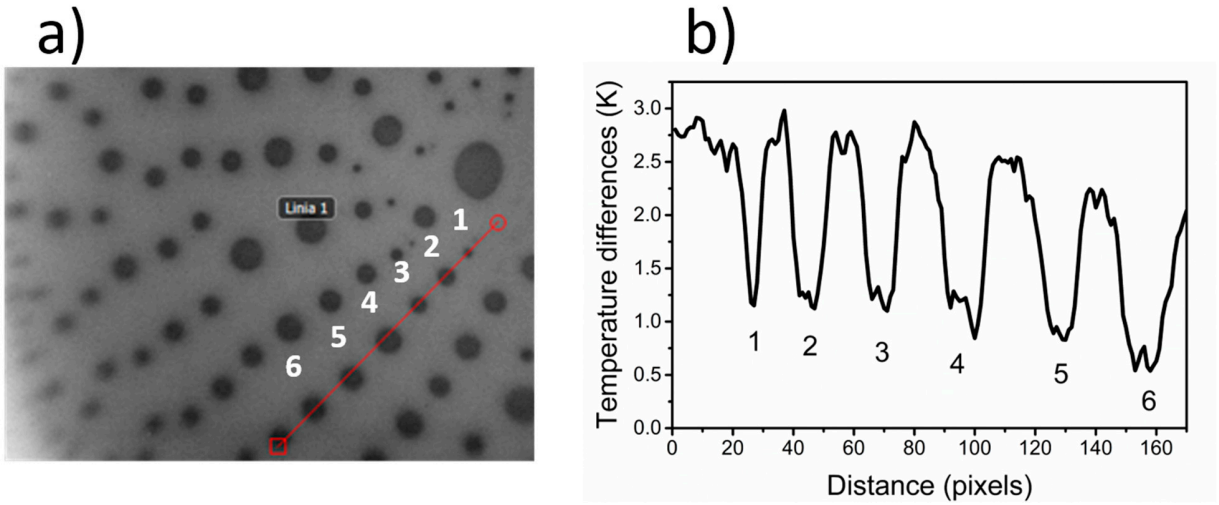

Figure S2. (a) A map of Marangoni bursting captured by thermal camera at the moment when mother droplet vanished. The red line was drawn across the 6 consecutive droplets detached from mother droplet. (b) Temperature differences measured along the red line. The temperature decrease at the position of each daughter droplet with respect to the oil surface amounts on average ($\Delta T \sim$ 1.3 K). Numbers serve for better visual correlation of the temperature changes on each droplet in a row. The length of the red line amounts in this case to about 20 mm.

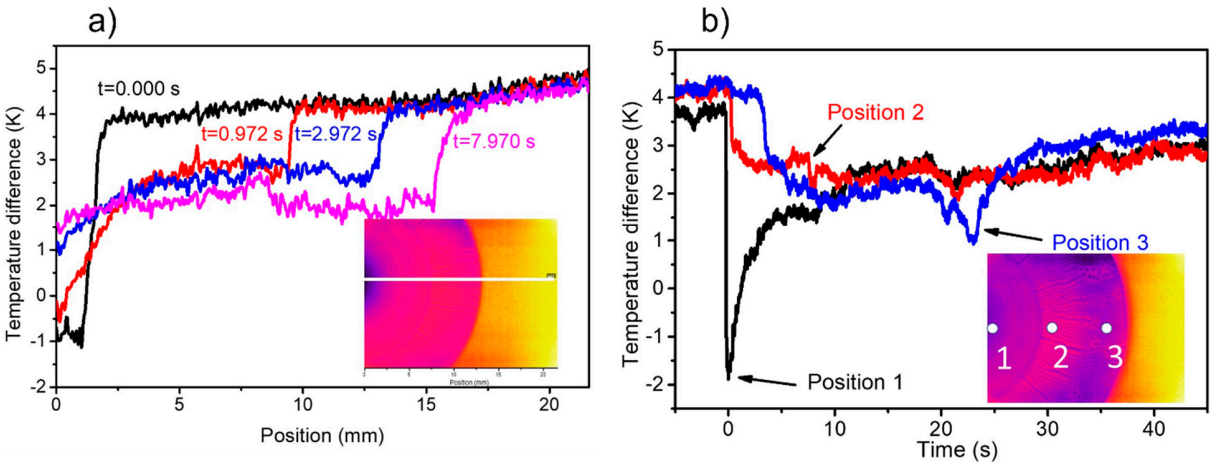

Figure S3. An example of analysis of kinetics of Marangoni bursting phenomenon in its expansion phase for IPA content in H_2O ϕ_0 = 0.7 (with methyl blue dye) on pure rapeseed oil via thermal camera FLIR E96. (a) Temperature difference along white line in function of time. (b) Evolution of local temperature changes measured in three different positions marked by white circles.

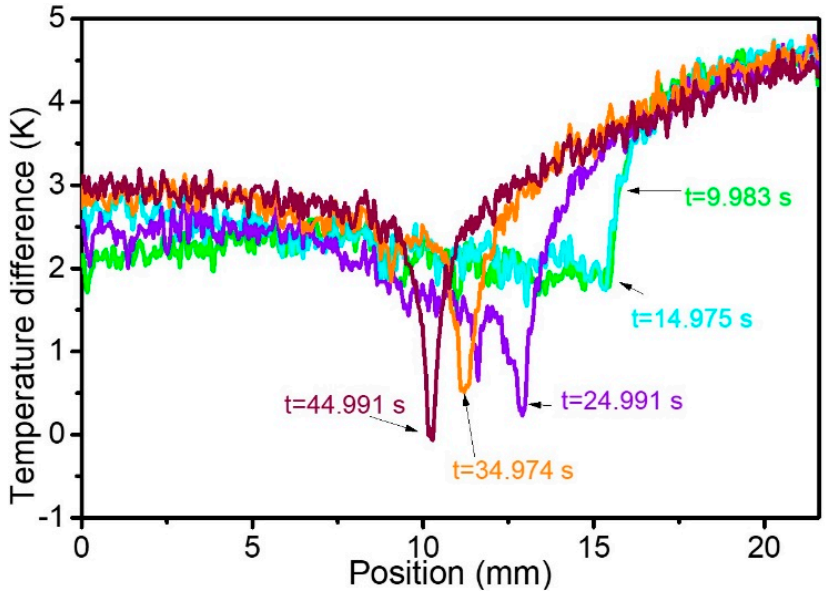

Figure S4. Analysis of kinetics of Marangoni bursting phenomenon in shrinking phase for IPA content in H_2O ϕ_0 = 0.7 with methyl blue dye on pure rapeseed oil via thermal camera FLIR E96. Temperature profiles were taken each 10 seconds, note that the temperature decrease at the surface is growing in time what suggests that the evaporation rate is approximately constant because the outer rim is moving slower.

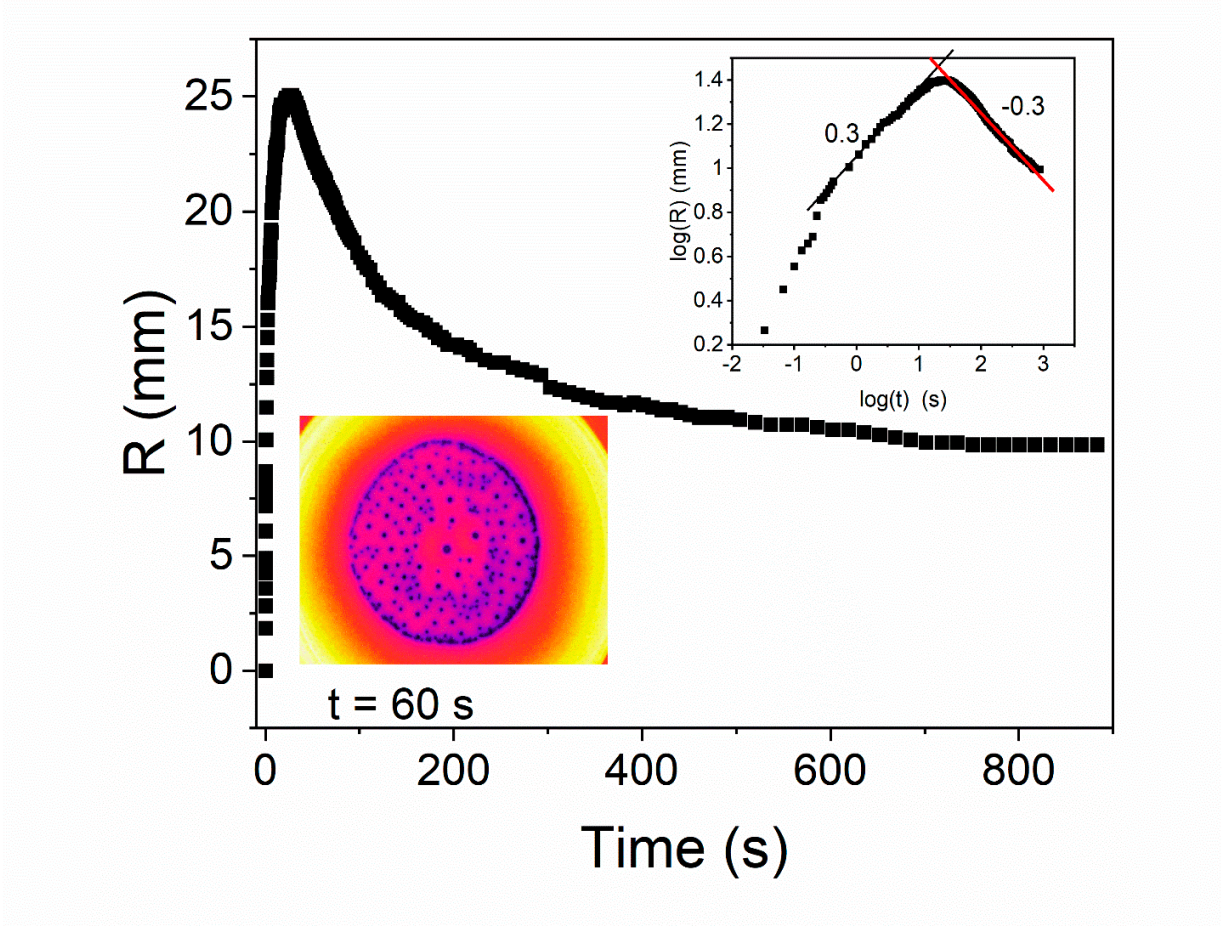

Figure S5. Analysis of kinetics of Marangoni bursting phenomenon in shrinking phase for IPA content in H_2O $\phi_0 = 0.5$ with methyl blue dye on pure rapeseed oil via thermal camera FLIR E96. Peripheric radius is plotted in function time. Inset shows the log(R(t)) versus log(t) plot showing power low dependence with $R(t) \propto t^n$ with n = + 0.3 during expansion period and with n' = − 0.3 during contraction phase.

For each studied initial binary solution IPA/water ϕ_0, the surface tension $\gamma_{mixture}$ has been measured separately with the conventional stalagmometry method. The results of these measurements performed at 295 K are shown in Figure S6. It can be noticed that for ϕ_0 (alcohol content in water)

in the range 35% to 80% surface tension changes within range of 28 – 25 mN/m. Surface tension of pure isopropyl alcohol amounts to 23 mN/m.

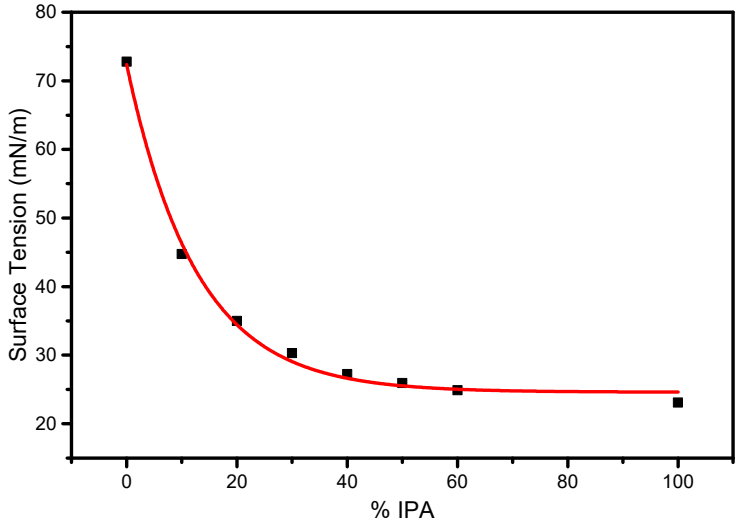

Figure S6. Surface tension $\gamma(\phi_0)$ of binary mixture IPA/water determined by stalagmometry method for different IPA fractions ϕ_0 in solution and measured at room temperature 295 K.

3. Parameters used in the simulations

Table S1. Rapeseed oil parameters used in simulations (oil contains 92 to 99% of triglycerides).

Name	Expression	Description
γ_T	-0.0000758[N/(m*K)]	Temperature derivative of the surface tension
ρ	910[kg/m^3]	Fluid density
μ	6.5e-4[Pa*s]	Dynamic viscosity
α_T	9.74e-8[m^2/s]	Thermal diffusivity
κ	0.180[W/(m*K)]	Thermal conductivity
C_p	2030[J/(kg*K)]	Heat capacity
α	1.3e-3[1/K]	Thermal expansion coefficient
T_{ref}	293.15 [K]	Reference temperature for material properties

Table S2. Chosen physicochemical properties of key substances involved in Marangoni bursting phenomenon at T = 293.15 K (taken from physicochemical data handbooks).

Property	**Demineralized water**	**Isopropyl alcohol, IPA**	**Rapeseed oil**	**Methyl blue dye**
Molecular formula	H_2O	C_3H_8O	92 to 99% triglycerides	$C_{37}H_{27}N_3Na_2O_9S_3$
Molar mass in g/mol	18.02	60.10	882	799.80
Density in g/cm^3	1.00	0.785	0.910	
Latent heat of vaporization J/g	2264.70	662.21		
Specific heat in J/g K	4.18	2.68		
Vapor pressure, at 293 K, kPa	2.34	4.40		
Dynamic viscosity mPa s	1.0005	2.37	0.65	
Kinematic viscosity, m^2/s	$1.0035x10^{-6}$	$3.08x10^{-6}$	$5x10^{-5}$	
Specific heat J/gK	4.18	1.54	2.030	
Thermal conductivity W/m K	0.6009	0.136	0.1666	
Surface tension, mN/m	71.99 72.8	23.00	31.3	
Surface tension temperature coefficient, mN/m K	-0.151	-0.078	-0.0758	

In Figure S7 we show results of simulations of thermocapillary Marangoni effect occurring in the oil pool whose surface temperature on the ring with a radius of r = 1 mm has been set to T = 288.15 K, i.e., 5 K below the room temperature. Simulations were performed within time period 0 – 4 s. We monitored evolution of surface temperature and surface Marangoni flow velocities u_x and u_z along the blue line that is positioned in oil phase close to the surface (see Figure S7a). The conditions of simulations correspond to the final stage of the Marangoni bursting phenomenon when on the surface is formed single circle composed of coalescing daughter droplets that still are colder than surrounding oil due to water evaporation that dominates in the final step. In Figure S7c one can observe the velocity of fluid in oil tending to shrink the circle. At the same time in Figure S7d there is observed a weak. flow of oil with component perpendicular to the oil pool surface. This flow transports the warmer oil toward the center and in this case elevating temperature in the

center of the pool. This makes that the velocities of fluid flow from the center toward periphery also exists and causing slower shrinking of the ring. Despite the fact that these simulations are only illustrative the physics connected with the final evolution of the ring is predicted with the agreement with experimental findings.

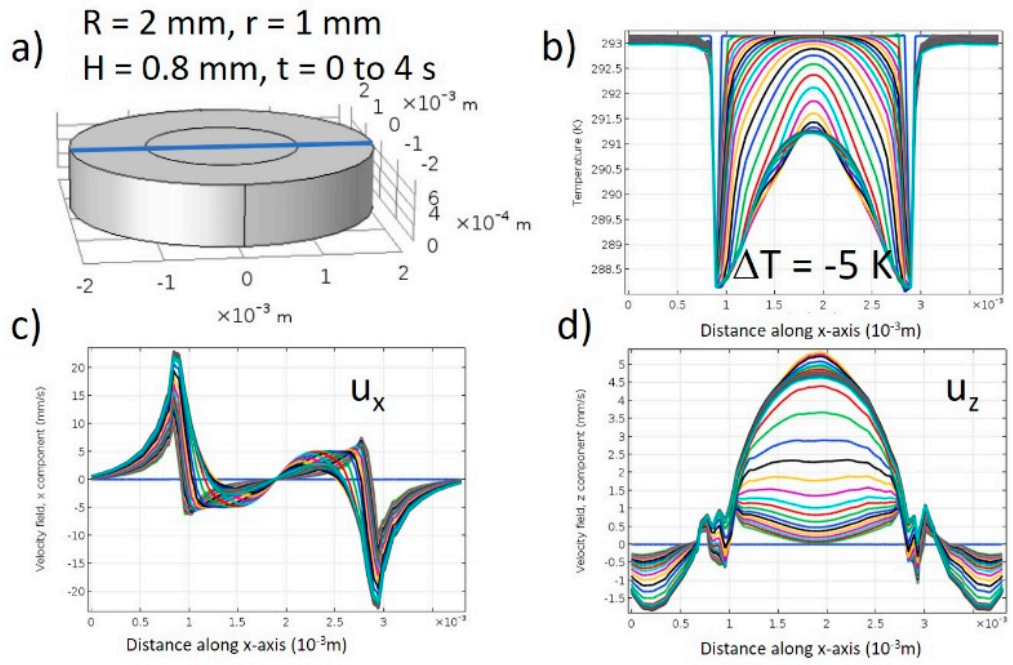

Figure S7. Simulations of thermocapillary Marangoni effect in the Marangoni bursting phenomenon in its very final step. (a) Oil bath with the thin cold ring at the surface and the cut line along the x-axis (blue line). (b) Temperature distribution for times from 0 to 4s. (c) Tangential velocities u_x of near surface flows along the x-axis within 0–4 s time range. (d) Velocity component u_z measured along the x-axis within 0–4 s time range. Color lines describe evolution in time of simulated parameters drawn in equal time periods of 200 ms from 0 to 4 s.

Acknowledgements

This work was financially supported by the National Science Centre, Poland, [grant UMO -2018/29/B/ST3/00829].